Stereocomplex crystallization and spherulite growth behavior of poly(L-lactide)-b-poly(D-lactide) stereodiblock copolymers

Hideto Tsuji*, Takeshi Wada, Yuzuru Sakamoto, Yu Sugiura

Department of Environmental and Life Sciences, Graduate School of Engineering, Toyohashi University of Technology, Tempaku-cho, Toyohashi, Aichi 441-8580, Japan

ABSTRACT

The non-isothermally and isothermally crystallized stereodiblock copolymers of poly(L-lactide) (PLLA) and poly(D-lactide) (PDLA) with equimolar L-lactyl and D-lactyl units and different number-average molecular weights (M_n) of 3.9×10^3, 9.3×10^3, and 1.1×10^4 g mol^{-1}, which are abbreviated as PLLA-b-PDLA copolymers, contained only stereocomplex crystallites as crystalline species, causing higher melting temperatures of the PLLA-b-PDLA copolymers compared to those of PLLA homopolymers. In the case of non-isothermal crystallization, the cold crystallization temperatures of the PLLA-b-PDLA copolymers during heating and cooling were respectively lower and higher than those of PLLA homopolymers, indicating accelerated crystallization of PLLA-b-PDLA copolymers. In the case of isothermal crystallization, in the crystallizable temperature range, the crystallinity (X_c) values of the PLLA-b-PDLA copolymers were lower than those of the PLLA homopolymers, and were susceptible to the effect of crystallization temperature in contrast to that of homopolymers. The radial growth rate of the spherulites (G) of the PLLA-b-PDLA copolymers was the highest at the middle M_n of 9.3×10^3 g mol^{-1}. This trend is different from that of the PLLA homopolymers where the G values increased monotonically with a decrease in M_n, but seems to be caused by the upper critical M_n values of PLLA and PDLA chains as in the case of PLLA/PDLA blends (in other papers), above which homo-crystallites are formed in addition to stereocomplex crystallites. The disturbed crystallization of PLLA-b-PDLA copolymers compared to that of the PLLA/PDLA blend is attributable to the segmental connection between the PLLA and PDLA chains, which interrupted the free movement of those chains of the PLLA-b-PDLA copolymers during crystallization. The crystallite growth mechanism of the PLLA-b-PDLA copolymers was different from that of the PLLA/PDLA blend.

© 2010 Elsevier Ltd. All rights reserved.

1. Introduction

Plant-derived poly(L-lactide), i.e., poly(L-lactic acid) (PLLA) is now produced from renewable corn starch and widely used as an alternative to petro-derived polymers to reduce the impact on the environment. The stereocomplexation between PLLA and poly(D-lactide) (PDLA) has been intensively studied because it can increase the mechanical performance and thermal/hydrolytic resistance of polylactide (PLA)-based materials [1–6]. Among the investigations, stereocomplex crystallization from the melt is a matter of concern in terms of processing the stereocomlexed PLA articles. The effects of molecular weight, polymer mixing ratio, optical purity, and processing conditions on the melt-crystallization of PLLA/PDLA and L-lactide-rich PLA/D-lactide-rich PLA blends were intensively investigated [1–6].

On the other hand, the synthesis of a wide variety of stereoblock copolymers of PLLA and PDLA has been carried out [7–19]. The segmental connection between PLLA and PDLA chains is thought to disturb stereocomplex crystallization due to restricted chain movement during crystallization. Despite the intensive studies, although the crystallization behavior of the stereoblock copolymers of PLLA and PDLA is crucial for their commodity production, only limited information has been accumulated. The exception is a report on the stereocomplex crystallization mechanism of PLLA and PDLA chains in the stereodiblock copolymers of PLLA and PDLA (PLLA-b-PDLA stereodiblock copolymers) having similar total number-average molecular weights (M_n) of 7.4–7.8×10^3 g mol^{-1}, and various L- and D-lactyl unit ratios during isothermal crystallization investigated by the use of wide-angle X-ray scattering (WAXS) and small-angle X-ray scattering [12].

In the present study, we synthesized the simplest stereoblock copolymers of PLLA and PDLA, i.e., PLLA-b-PDLA stereodiblock copolymers having equimolar L- and D-lactyl units and different total M_n values of 3.9×10^3–1.1×10^4 g mol^{-1}, and investigated in

detail their isothermal and non-isothermal crystallization by the use of differential scanning calorimetry (DSC), WAXS, and polarized optical microscopy (POM). The thus obtained results were compared with those of PLLA homopolymers and the PLLA/PDLA blend, and the effect of the molecular weight of the equimolar PLLA-b-PDLA stereodiblock copolymers on crystallization kinetics and the final crystalline state is discussed.

2. Experimental part

2.1. Materials

The synthesis of PLLA-b-PDLA copolymers was performed as follows, according to the procedure reported by Yui et al. [7]. That is, relatively, low-molecular-weight PLLA prepolymers were synthesized by ring-opening polymerization of L-lactide in the presence of stannous octoate (0.03 wt% of L-lactide) and L-lactic acid as the initiator and coinitiator, respectively, at 140 °C for 10 h [20]. The L-lactide/L-lactic acid ratios (mol/mol) were 7/1, 21/1, 42/1, 63/1, and 84/1 and the L-lactic acid used was obtained by hydrolysis of L-lactide with a theoretical amount of distilled water [L-lactide/water(mol/mol) = 1/2]. For reference, PLLA and PDLA were synthesized by ring-opening polymerization of L-lactide and D-lactide in the presence of L-lactic acid and D-lactic acid as coinitiators. The synthesized polymers were purified using chloroform and methanol as the solvent and non-solvent, respectively. The purified polymers were dried under reduced pressure for at least 7 days. Each dried PLLA prepolymer, D-lactide [PLLA/D-lactide (w/w) = 1/1], and stannous octoate (0.03 wt% of D-lactide) was dissolved in toluene, sealed in a test tube, and then ring-opening polymerization of D-lactide was performed at 120 °C for 24 h. Each dried PLLA prepolymer had M_n of 1.7, 3.0, and 6.2 × 10^3 g mol^{-1} and was respectively abbreviated as PLLA2, PLLA3, and PLLA6. The obtained PLLA-b-PDLA copolymers, which became insoluble in toluene at room temperature, were removed from toluene, dissolved in a mixed solvent of chloroform/1,1,1,3,3,3-hexafluoro-2-propanol (vol/vol = 95/5), and then precipitated in methanol. The thus purified stereodiblock copolymers were dried in the same way as for the PLLA homopolymers. For preparation of melt-quenched and crystallized specimens, each PLLA homopolymer or PLLA-b-PDLA copolymer packed in a DSC aluminum cell was sealed in a test tube under reduced pressure, melted at 200 °C (PLLA homopolymers) and 250 °C (PLLA-b-PDLA copolymers) in a thermostatically controlled oil bath for 3 min, and quenched at 0 °C in iced water for 5 min (melt-quenched specimens), or crystallized at a predetermined crystallization temperature (T_c) of 100–190 °C for 10 h,

and quenched at 0 °C for 5 min (isothermally crystallized specimens). The specimen temperature in a test tube at room temperature reaches 190 and 240 °C in an oil bath at 200 and 250 °C, respectively, within 20 s, and finally 200 and 250 °C within 45 s. The specimen temperature in a test tube at 200 and 250 °C reaches 10 °C in iced water of 0 °C within 30 s, and finally 5 °C within 45 s. We confirmed that these time lags never caused imperfect melting during heating, or crystallization during quenching.

2.2. Physical measurements and observation

The weight-average molecular weight (M_w) and M_n of the specimens were evaluated in chloroform at 40 °C with a Tosoh (Tokyo, Japan) GPC system (refractive index monitor: RI-8020) with two TSK Gel columns (GMH$_{xL}$) using polystyrene standards. For the preparation of GPC sample solutions of PLLA-b-PDLA copolymers, the mixture of chloroform and 1,1,1,3,3,3-hexafluoro-2-propanol (vol/vol = 95/5) was used as the solvent, whereas in the case of PLLA homopolymers, only chloroform was used as the solvent. The specific optical rotation ($[\alpha]_{25}^{589}$) of the polymers was measured in chloroform at a concentration of 1 g dL^{-1} and 25 °C using a JASCO (Tokyo, Japan) P-2100 polarimeter at a wave length of 589 nm. The L-lactyl unit content of the PLLA-b-PDLA copolymers is estimated by the following equation:

$$L - lactyl\ unit\ content\ (\%) = 100 \times \left\{ [\alpha]_{25}^{589} + [\alpha]_{25}^{589}(PLLA) \right\} \Big/ \left\{ 2 \times [\alpha]_{25}^{589}(PLLA) \right\} \quad (1)$$

where $[\alpha]_{25}^{589}(PLLA)$ is the $[\alpha]_{25}^{589}$ value for the PLLA homopolymer used for the synthesis of the PLLA-b-PDLA copolymer. The evaluated molecular characteristics are shown in Table 1.

In regard to the glass transition, cold crystallization, and melting temperatures (T_g, T_{cc}, and T_m, respectively) and the enthalpies of the melting of the homo-crystallites and stereo-complex crystallites [ΔH_m(H) and ΔH_m(S), respectively], the specimens were determined by a Shimadzu (Kyoto, Japan) DSC-50 differential scanning calorimeter with a cooling cover (LTC-50) under a nitrogen gas flow of 50 mL min^{-1}. For monitoring the crystallization during heating, the melt-quenched specimens were heated from room temperature to 230 °C at a rate of 10 °C min^{-1} (DSC data was obtained here). For tracing the crystallization during cooling from the melt, the specimens were heated from room temperature to 250 °C at a rate of 30 °C min^{-1}, melted at the same temperature for 1 min, and then cooled at −3 °C min^{-1} to room temperature (DSC data was also obtained here). The T_g, T_{cc}, T_m, ΔH_m(H), and ΔH_m(S) of the

Table 1
Characteristics and thermal properties of PLLA homopolymers and PLLA-b-PDLA copolymers synthesized in the present study.

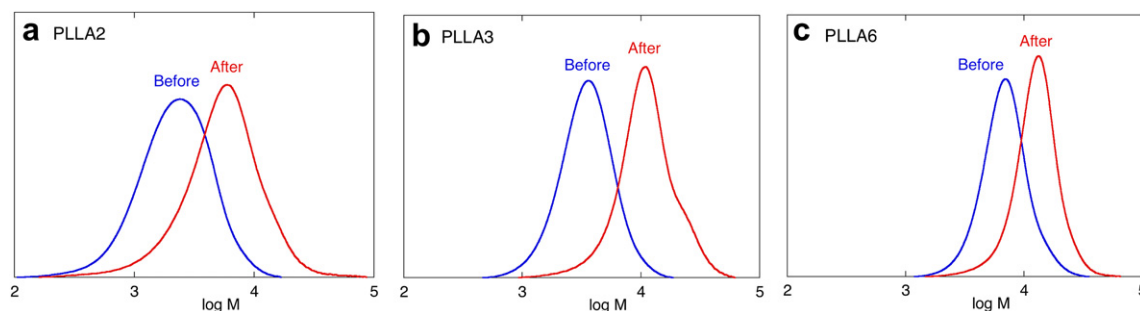| Code [a]	Coinitiator	Lactide/Coinitiator (mol/mol) or (w/w)	Polymer			
			M_n[b](g mol^{-1})	M_w/M_n[b]	$[\alpha]_{25}^{589}$ [c] (deg dm^{-1} g^{-1} cm^3)	L-lactyl unit content (%)
PLLA2	L-lactic acid	7[d]	1.7 × 10^3	1.6	−161	−
PLLA3		21[d]	3.0 × 10^3	1.3	−165	−
PLLA6		42[d]	6.2 × 10^3	1.2	−167	−
PLLA9		63[d]	8.7 × 10^3	1.2	−169	−
PLLA14		84[d]	1.4 × 10^4	1.4	−171	−
PLLA-b-PDLA4	PLLA2	1[e]	3.9 × 10^3	1.8	0	50.0
PLLA-b-PDLA9	PLLA3		9.3 × 10^3	1.4	−5	51.5
PLLA-b-PDLA11	PLLA6		1.1 × 10^4	1.2	−3	50.9

[a] The figure following the letters indicates the M_n value/10^3.
[b] M_n and M_w are number- and weight-average molecular weights, respectively.
[c] Specific optical rotation.
[d] In mol/mol.
[e] In w/w.

Fig. 1. GPC curves of PLLA2 (a), PLLA3 (b), and PLLA6 (c) before and after second polymerization of D-lactide. Here, PLLA2, PLLA3, and PLLA6 after polymerization of D-lactide are PLLA-*b*-PDLA3, PLLA-*b*-PDLA9, and PLLA-*b*-PDLA11, respectively.

specimens were calibrated using tin, indium, and benzophenone as standards. In the present study, T_{cc} is defined as a peak temperature.

The crystallinity of the stereocomplex and homo-crystallites [X_c(S) and X_c(H), respectively] in isothermally crystallized specimens were estimated by the use of WAXS. The WAXS measurements were performed at 25 °C using a RINT-2500 equipped with a Cu-K$_\alpha$ source ($\lambda = 0.1542$ nm), which was operated at 40 kV and 200 mA (Rigaku Co., Tokyo, Japan). Namely, in a *2θ* range of 10–25°, the crystalline peak areas for stereocomplex crystallites at *2θ* values of 12, 21, and 24° and for homo-crystallites at *2θ* values of 15, 17, 19° and so on relative to the total area between a diffraction profile and a baseline were used to estimate X_c(S) and X_c(H), respectively [3,21]. We did not calculate crystallinity from DSC results, because stereocomplex crystallites are formed during DSC heating, as reported previously [22], which disturbs accurate evaluation of X_c(S) and X_c(H).

Spherulite growth in the PLLA homopolymers and the PLLA-*b*-PDLA copolymers was observed by an Olympus (Tokyo, Japan) polarization optical microscope (BX50) equipped with a heating–cooling stage and temperature controller (LK-600PM, Linkam Scientific Instruments, Surrey, UK) under a constant nitrogen gas flow. The PLLA homopolymers and the PLLA-*b*-PDLA copolymers were first heated from room temperature to 200 and 250 °C, respectively, at 100 °C min^{-1}, held at the same temperature for 3 min, cooled to an arbitrary T_c in the range of 100–190 °C at 100 °C min^{-1}, and then held at the T_c (spherulite growth was observed here).
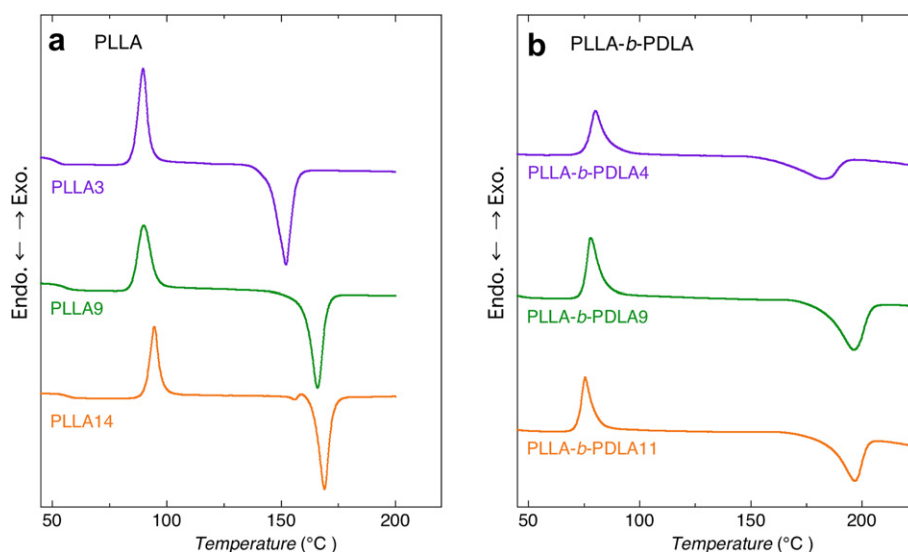
3. Results and discussion

3.1. Synthesis of PLLA-b-PDLA

The PLLA-*b*-PDLA copolymers were synthesized by a previously reported procedure [7]. Fig. 1 shows the GPC curves of the three PLLA prepolymers before and after the second polymerization of D-lactide. Evidently, the molecular weight distribution curves of the PLLA prepolymers as coinitiators shifted to higher molecular weights after D-lactide polymerization. This figure indicates that PDLA chain grew from the PLLA coinitiators, and as a result stereodiblock copolymers of PLLA and PDLA, i.e., PLLA-*b*-PDLA copolymers were formed. The molecular characteristics of the synthesized PLLA-*b*-PDLA copolymers are summarized in Table 1. The L-lactyl unit content of the PLLA-*b*-PDLA copolymers estimated from $[\alpha]_{25}^{589}$ is around 50%, indicating that the PLLA-*b*-PDLA copolymers contained equimolar L-lactyl and D-lactyl units.

3.2. Non-isothermal crystallization

3.2.1. During heating

Fig. 2 shows the DSC thermograms of melt-quenched PLLA homopolymers and PLLA-*b*-PDLA copolymers during heating. The glass transition peak, cold crystallization peak, and melting peaks of homo-crystallites and stereocomplex crystallites are observed at 40–60, 70–100, 150–170, and 170–200 °C. For all of the PLLA-*b*-PDLA copolymers, melting peaks (the temperatures of which were

Fig. 2. DSC thermograms of melt-quenched PLLA homopolymers (a) and PLLA-*b*-PDLA copolymers (b) during heating.

Table 2
Thermal properties of melt-quenched PLLA homopolymers and PLLA-b-PDLA copolymers during heating from room temperature, and as-purified PLLA homopolymers and PLLA-b-PDLA copolymers during cooling from the melt.

Code	Heating					Cooling	
	T_g^a (°C)	T_{cc}^a (°C)	T_m^a (°C)	ΔH_{cc}^b (J g^{-1})	ΔH_m^b (J g^{-1})	T_{cc}^a (°C)	ΔH_{cc}^b (J g^{-1})
PLLA3	47.9	89.5	152.1	57.8	58.0	109.4	43.3
PLLA9	51.6	89.9	165.9	56.1	54.0	107.7	49.7
PLLA14	53.4	94.6	169.0	42.3	42.0	109.6	49.4
PLLA-b-PDLA4	36.1	80.1	182.1	35.4	33.9	124.5	44.8
PLLA-b-PDLA9	38.5	77.9	196.2	54.4	55.1	141.4	47.7
PLLA-b-PDLA11	38.6	75.5	196.7	40.7	41.1	137.5	46.8
PLLA7/PDLA7	46.1	78.8	219.7	63.3	65.1	189.1	111.5

[a] T_g, T_{cc}, and T_m are glass transition, cold crystallization, and melting temperatures, respectively.
[b] ΔH_{cc} and ΔH_m are cold crystallization and melting enthalpies, respectively.

20–30 °C higher than those of the PLLA homopolymers) were observed, indicating that during heating only stereocomplex crystallites as crystalline species were formed. With an increase in molecular weight, although the cold crystallization peaks of the PLLA homopolymers and the PLLA-b-PDLA copolymers shifted slightly, the melting peaks shifted to significantly higher temperatures.

The T_g, T_{cc}, T_m, and ΔH_{cc} values were estimated from Fig. 2 and the thus obtained values are tabulated in Table 2. The T_g values of the PLLA-b-PDLA copolymers were lower than those of the PLLA homopolymers, probably due to the presence of a connecting point between segments with different configurations in a molecule, which may have disturbed the dense packing of the segments. On the other hand, due to the stereocomplex formation, the T_m values of the PLLA-b-PDLA copolymers were higher than those of the PLLA homopolymers. The T_m values of the PLLA-b-PDLA copolymers (182–197 °C) in the present study are lower than the 205 °C reported for PLLA-b-PDLA with a higher M_n of 2.0×10^4 g mol^{-1} [7] and are comparable with or lower than the 196–218 °C of well-defined stereomultiblock copolymers having similar or higher M_n values of 1.4–5.7 $\times$ 10^4 g mol^{-1} [15], but higher than the 110–140 °C of relatively random stereomultiblock copolymers with similar M_n values of 7.1×10^3 and 1.1×10^4 g mol^{-1} [10]. The T_{cc} values were lower for the PLLA-b-PDLA copolymers (76–80 °C) than for the PLLA homopolymers (90–95 °C), indicating the higher crystallizability of the PLLA-b-PDLA copolymers during heating. The ΔH_{cc} values were higher for the PLLA homopolymers than for

the PLLA-b-PDLA copolymers in M_n ranges below and above 9×10^3 g mol^{-1}, respectively.

To obtain the T_g and T_m values of the PLLA homopolymers and the PLLA-b-PDLA copolymers at infinite molecular weight (T_g^∞ and T_m^∞, respectively), the T_g and T_m^{-1} values are plotted in Fig. 3 as a function of M_n^{-1} according to the Flory–Fox [23] and Flory [24] equations, respectively:
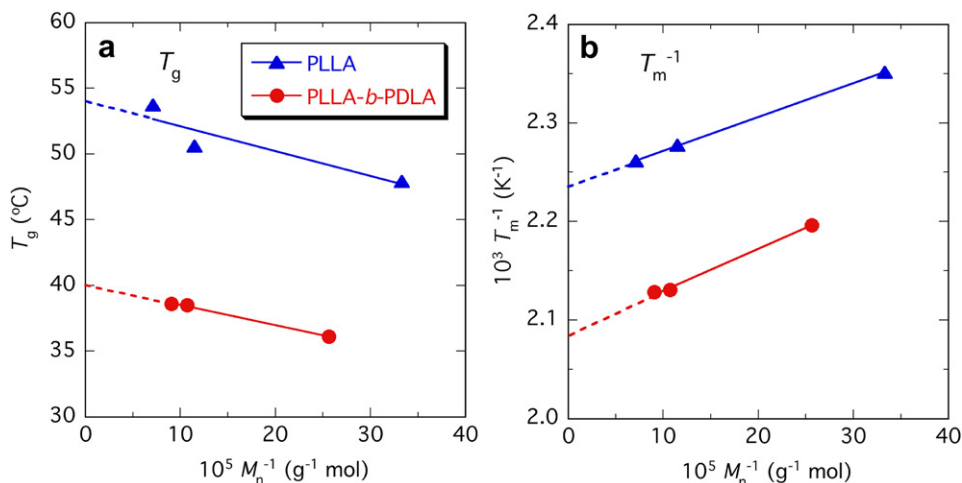
$$T_g = T_g^\infty - K/M_n \qquad (2)$$

$$T_m^{-1} = (T_m^\infty)^{-1} - 2R\,M_0/(\Delta H_m\,M_n), \qquad (3)$$

where K is a constant representing the excess free volume of the end groups of the polymer chains, M_0 is the molecular weight of a half lactide unit (72.1 g mol^{-1}), and R is the gas constant. The T_g^∞ values estimated using eq. (2) from Fig. 3(a) were 54.0 and 40.1 °C for the PLLA homopolymers and the PLLA-b-PDLA copolymers, respectively, suggesting that block copolymerization of L- and D-lactide increases the chain mobility of PLA even at infinite M_n. The estimated T_g^∞ value for the PLLA homopolymers is in agreement with the 58 °C reported by Jamshidi et al. for PLLA [25], whereas that for the PLLA-b-PDLA copolymers was much lower. The K values evaluated using eq. (2) from Fig. 4(a) were 1.9×10^4 and 1.6×10^4 K g mol^{-1} for the PLLA homopolymers and the PLLA-b-PDLA copolymers, respectively, reflecting the similar excess free volume of the terminal groups of the PLLA homopolymers and the PLLA-b-PDLA copolymers. However, the evaluated K values for the PLLA homopolymers and the PLLA-b-PDLA copolymers are lower than the 5.5×10^5 K g mol^{-1} reported for PLLA [25]. On the other hand, the T_m^∞ values obtained using eq. (3) from Fig. 3(b) were 174 and 206 °C for the PLLA homopolymers and PLLA-b-PDLA copolymers, respectively. The estimated T_m^∞ value for the PLLA-b-PDLA copolymers is much lower than the T_m values reported for PLLA/PDLA blends (ca. 230 °C) and the estimated T_m^∞ value for the PLLA homopolymers is lower than the reported value (184 °C) [25].

3.2.2. During cooling

Fig. 4 shows the DSC thermograms of the PLLA homopolymers and the PLLA-b-PDLA copolymers during cooling from the melt. The T_{cc} and ΔH_{cc} values were estimated from Fig. 4 and the thus obtained values are summarized in Table 2. Although the abbreviation T_{cc} is not preferable for the cooling process, we use it to distinguish it from the T_c used for isothermal crystallization. The T_{cc}

Fig. 3. T_g (a) and T_m^{-1} (b) of melt-quenched PLLA homopolymers and PLLA-b-PDLA copolymers during heating as a function of reciprocal of M_n^{-1}.

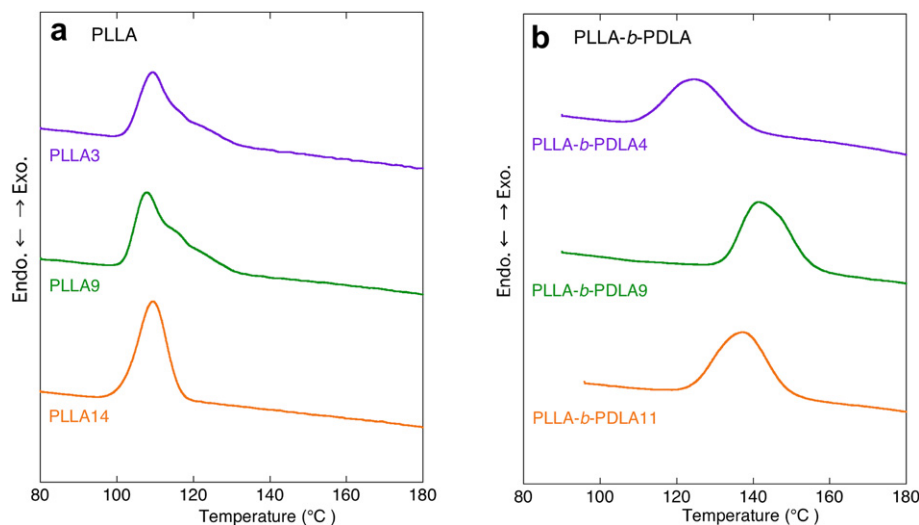**Fig. 4.** DSC thermograms of PLLA as-purified homopolymers (a) and PLLA-*b*-PDLA copolymers (b) during cooling from the melt.

values were higher for the PLLA-*b*-PDLA copolymers than for the PLLA homopolymers. This is attributable to the higher T_m values of the PLLA-*b*-PDLA copolymers (180–200 °C), which increase the supercooling ($\Delta T = T_m - T_c$) during cooling compared to those of the PLLA homopolymers (150–170 °C). The difference in T_{cc} between the PLLA-*b*-PDLA copolymers and the PLLA homopolymers becomes smaller with a decrease in M_n. On the other hand, the ΔH_{cc} values of the PLLA-*b*-PDLA copolymers and the PLLA homopolymers were similar to each other and constant at around 50 J g^{-1}, irrespective of the molecular weight.

3.3. Isothermal crystallization

3.3.1. Wide-angle X-ray scattering
Fig. 5 shows the typical WAXS profiles of the PLLA9 homopolymer and the PLLA-*b*-PDLA9 copolymer crystallized at different T_c values from the melt. The crystalline diffraction peaks of $2\theta = 15, 17, 19°$, and so on in Fig. 5(a) are ascribed to those of the α- or α′-form of PLLA, whereas the crystalline diffraction peaks of $2\theta = 12, 21$, and $24°$ in Fig. 5(b) are attributed to those of the stereocomplex

crystalline form. Although Fig. 5 shows typical data, the WAXS profiles indicated that the PLLA homopolymers crystallized in the α- or α′-form in T_c ranges of 100–140, 100–150, and 100–150 °C for PLLA3, PLLA9, and PLLA14 [26], whereas the PLLA-*b*-PDLA copolymers crystallized only in the stereocomplex crystalline form (not in the α- nor α′-form) in T_c ranges of 110–170, 110–180 and 110–180 °C for PLLA-*b*-PDLA4, PLLA-*b*-PDLA9, and PLLA-*b*-PDLA11.

3.3.2. Differential scanning calorimetry
Fig. 6 shows the typical DSC thermograms of the PLLA9 homopolymer and the PLLA-*b*-PDLA9 copolymer crystallized at different T_c values from the melt. The X_c and T_m of the crystallized PLLA homopolymers and PLLA-*b*-PDLA copolymers were estimated from the WAXS and DSC data and are plotted in Fig. 7 as a function of T_c. When a double melting peak is observed, the first peak temperature is assumed to be T_m, because the second melting peak should be ascribed to the melting of re-crystallized crystallites formed during heating. Most X_c and T_m values of the PLLA homopolymers and the PLLA-*b*-PDLA copolymers increased with an increase in T_c and gave maximum values in the T_c range of 120–150 °C and
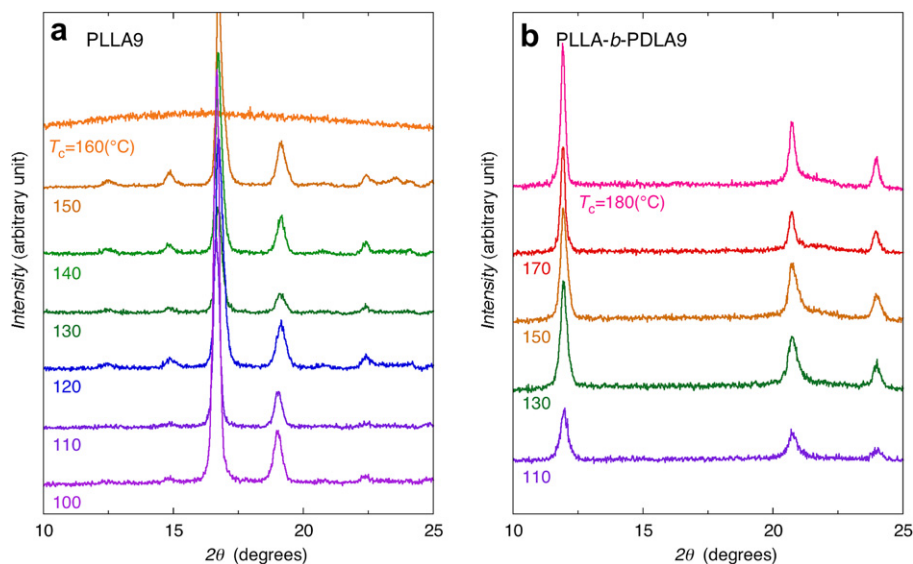

Fig. 5. Wide-angle X-ray scattering profiles of PLLA9 homopolymer (a) and PLLA-*b*-PDLA9 copolymer (b) crystallized at different crystallization temperatures (T_c) from the melt.
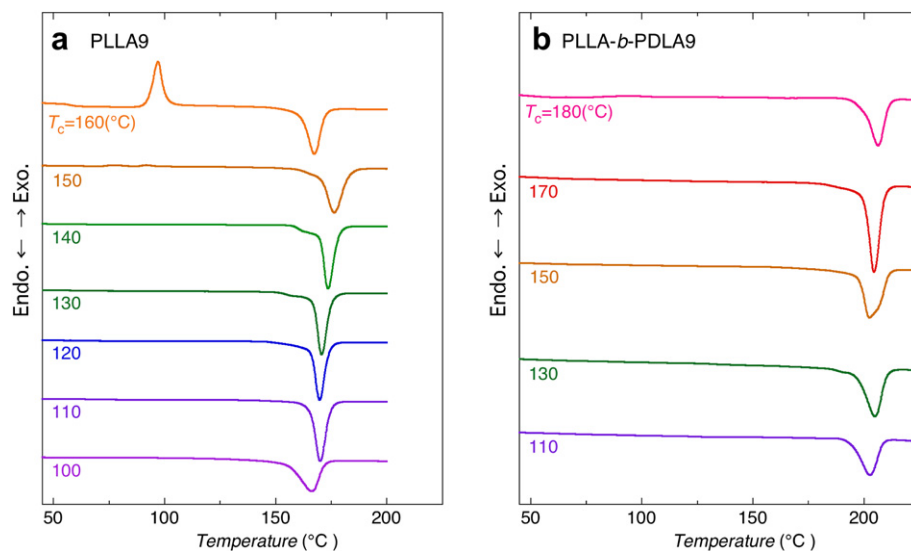
Fig. 6. DSC thermograms of PLLA9 (a) and PLLA-*b*-PDLA9 (b) crystallized at different T_{cc} from the melt.

170–180 °C, respectively, excluding the X_c of the PLLA-*b*-PDLA4 copolymer, which decreased monotonically with an increase in T_c. Such a difference in T_c, giving maximum X_c and T_m values between the PLLA homopolymers and the PLLA-*b*-PDLA copolymers, can be attributed to the higher T_m values of the PLLA-*b*-PDLA copolymers compared to those of the PLLA homopolymers. X_c was nil and T_m decreased when T_c approached T_m. The average X_c values of the PLLA-*b*-PDLA copolymers were lower than those of the PLLA
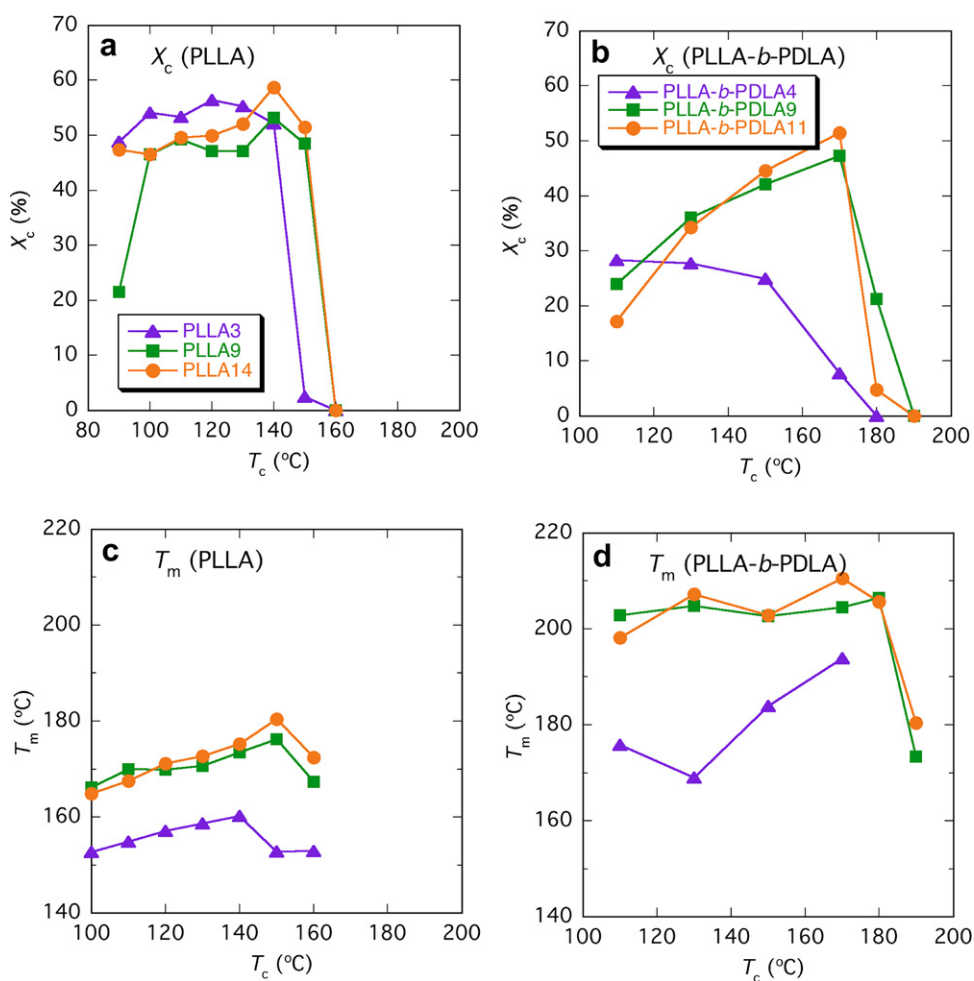

Fig. 7. Crystallinity (X_c) (a,b) and T_m (c,d) of PLLA homopolymers (a,c) and PLLA-*b*-PDLA copolymers (b,d) as a function of T_c.
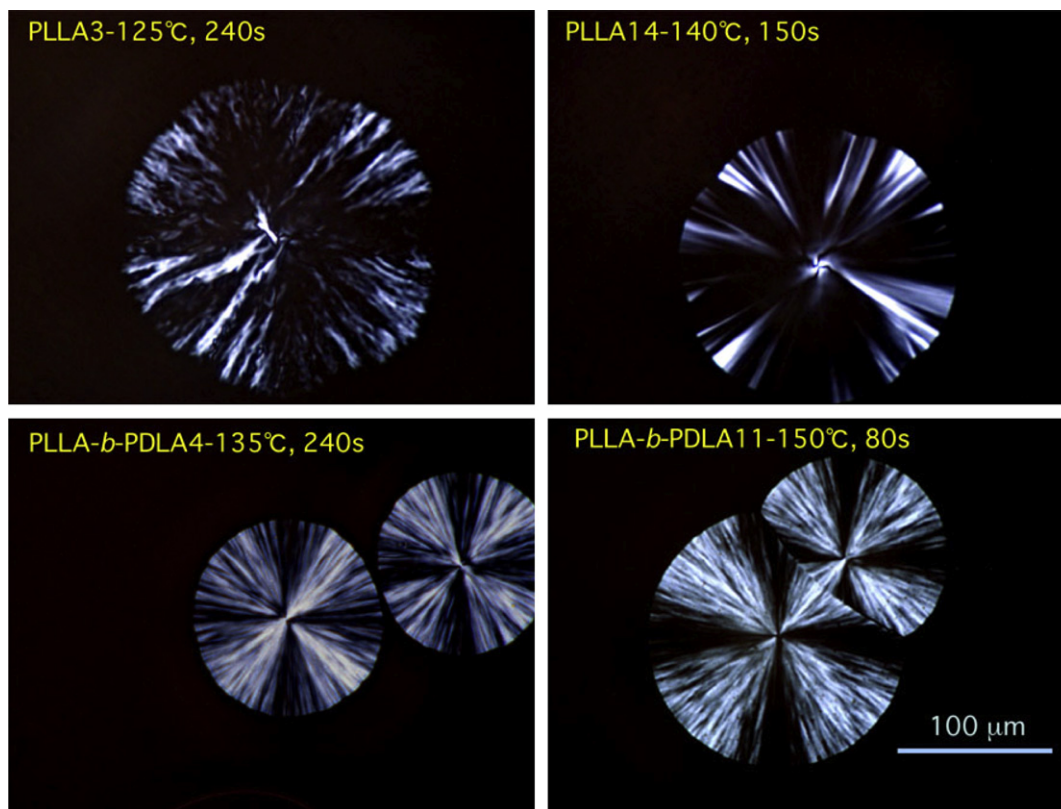
Fig. 8. Polarized optical photomicrographs of PLLA3 and PLLA14 homopolymers plus PLLA-*b*-PDLA4 and PLLA-*b*-PDLA11 copolymers crystallized at shown T_c and time.
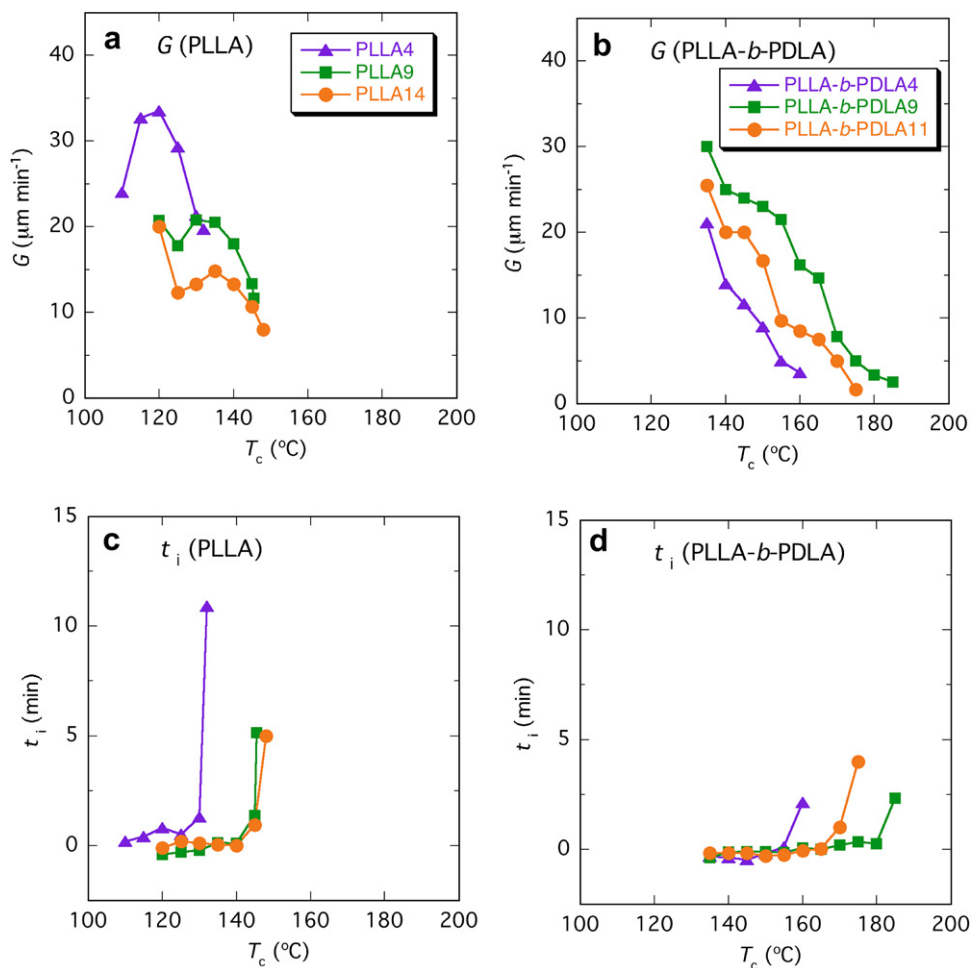
homopolymers, whereas due to the stereocomplex formation, the average T_m values of the PLLA-*b*-PDLA copolymers were higher than those of the PLLA homopolymers. In the crystallizable T_c range, the effect of T_c on X_c was more remarkable for the PLLA-*b*-PDLA copolymers than for the PLLA copolymers. The crystallization of the PLLA-*b*-PDLA4 copolymer, having the lowest molecular weight as traced by X_c and T_m, was disturbed compared to the PLLA-*b*-PDLA9 and PLLA-*b*-PDLA11 copolymers with higher molecular weights.

The equilibrium melting temperature (T_m^0) of the PLLA homopolymers and the PLLA-*b*-PDLA copolymers was estimated from the Hoffman–Weeks procedure. This procedure may give T_m^0 values slightly different from real T_m^0 values, as suggested by Alamo et al. [27] and Marand et al. [28]. However, we have used this simple procedure to obtain approximate T_m^0 values, since the difference between the values using this procedure (478–485 K) and the Gibbs–Thomson equation (478 K) was very small for linear PLLA [29]. The T_m^0 values of the PLLA homopolymers and the PLLA-*b*-PDLA copolymers were estimated using the linear parts of T_m data. The T_m data used were those in the T_c ranges of 100–140, 100–150, and 100–150 °C for the PLLA3, PLLA9, and PLLA14 homopolymers and of 130–170, 110–180, and 110–180 °C for the PLLA-*b*-PDLA4, PLLA-*b*-PDLA9, and PLLA-*b*-PDLA11 block copolymers. The T_m^0 values obtained for the PLLA3, PLLA9, and PLLA14 homopolymers were 164.6, 179.4, and 188.9 °C, respectively, which are comparable with or lower than the reported values of 191–227 °C [29–34]. This is attributable to the low molecular weights of the PLLA homopolymers utilized in the present study, which should have reduced the upper limit of the crystalline thickness and increased the surface energy effect of the PLLA crystalline regions. The T_m^0 values obtained for the PLLA-*b*-PDLA4, PLLA-*b*-PDLA9, and PLLA-*b*-PDLA11 copolymers were 235.4, 206.3, and 211.8, respectively. These values are much lower than the T_m^0 value estimated for PLLA/PDLA blends (279 °C) [35], but are comparable with or lower than those

estimated by using stereocomplex crystalline residues hydrolyzed at different times and therefore having different thicknesses (233–237 °C) [36].
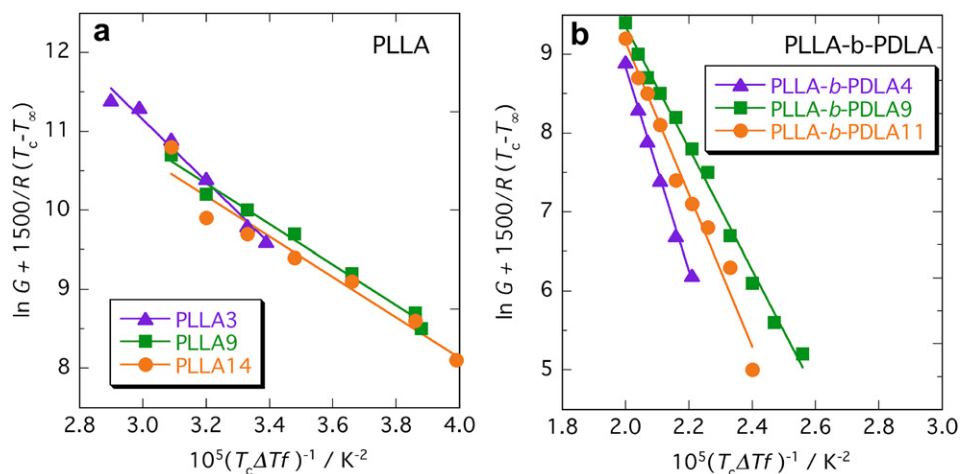
3.3.3. Polarized optical microscopy

Fig. 8 shows the typical polarized optical photomicrographs of the PLLA3 and PLLA14 homopolymers and the PLLA-*b*-PDLA4 and PLLA-*b*-PDLA11 copolymers. In the cases of the PLLA homopolymers PLLA3 and PLLA14, rather disordered spherulites were formed, whereas the spherulites of the block copolymers PLLA-*b*-PDLA4 and PLLA-*b*-PDLA11 had well-defined Maltese crosses. This indicates that the crystalline regions in the stereocomplex spherulites of the PLLA-*b*-PDLA copolymers were well oriented along the radial direction. Fig. 9 shows the radial growth rate of the spherulites (G) and the induction period for spherulite growth (t_i) of the PLLA homopolymers and the PLLA-*b*-PDLA copolymers. Although the G values of the PLLA-*b*-PDLA copolymers cannot be compared with those of the PLLA homopolymers for a wide T_c range due to the difference in the traceable T_c range for G, the G values of the PLLA-*b*-PDLA copolymers were higher than those of the PLLA homopolymers when compared at the same T_c. The G values increased with a decrease in molecular weight, whereas the G values of the PLLA-*b*-PDLA copolymers became maximum at the middle M_n of 9.3×10^3 g mol^{-1}. The former indicates that the G values of the PLLA homopolymers are determined mainly by the molecular weight or molecular mobility. However, the latter reflects the fact that the molecular weight is not the sole factor which determines the G values. In the case of PLLA/PDLA blends (in other papers), homo-crystallites, in addition to stereocomplex crystallites, are formed when the molecular weights of PLLA and PDLA are increased over the upper critical values, and in a molecular weight range of over 2×10^5 g mol^{-1} only homo-crystallites are formed [3]. This is due to the size of the PLLA or PDLA chains

Fig. 9. Radial growth rate of spherulites (*G*) (a,b) and induction period for spherulite growth (t_i) (c,d) of PLLA homopolymers (a,c) plus PLLA-*b*-PDLA copolymers (b,d) crystallized from the melt as a function of T_c.

(too large), which reduces the fraction of the domain composed of equimolar PLLA and PDLA chains and consequently disturbs the ready formation of the stereocomplex crystallites. It is probable also in the case of PLLA-*b*-PDLA block copolymers, that a molecular weight of block copolymers which is too high increases the domain sizes of the PLLA chain or PDLA chain, resulting in delayed stereocomplex crystallization. On the other hand, the t_i of the PLLA homopolymers and the PLLA-*b*-PDLA copolymers increased from nil to a significant value when T_c approached T_m. Therefore, the T_c above at which the t_i has a non-zero value was greater for the PLLA-*b*-PDLA copolymers with relatively high T_m values than for the PLLA homopolymers having relatively low T_m values.

Fig. 10. ln *G* + 1500/$R(T_c$-$T_\infty)$ of PLLA homopolymers (a) and PLLA-*b*-PDLA copolymers (b) as a function of $1/(T_c\Delta Tf)$.

Table 3
Front constant (G_o) and nucleation constant (K_g) of PLLA homopolymers and PLLA-*b*-PDLA copolymers.

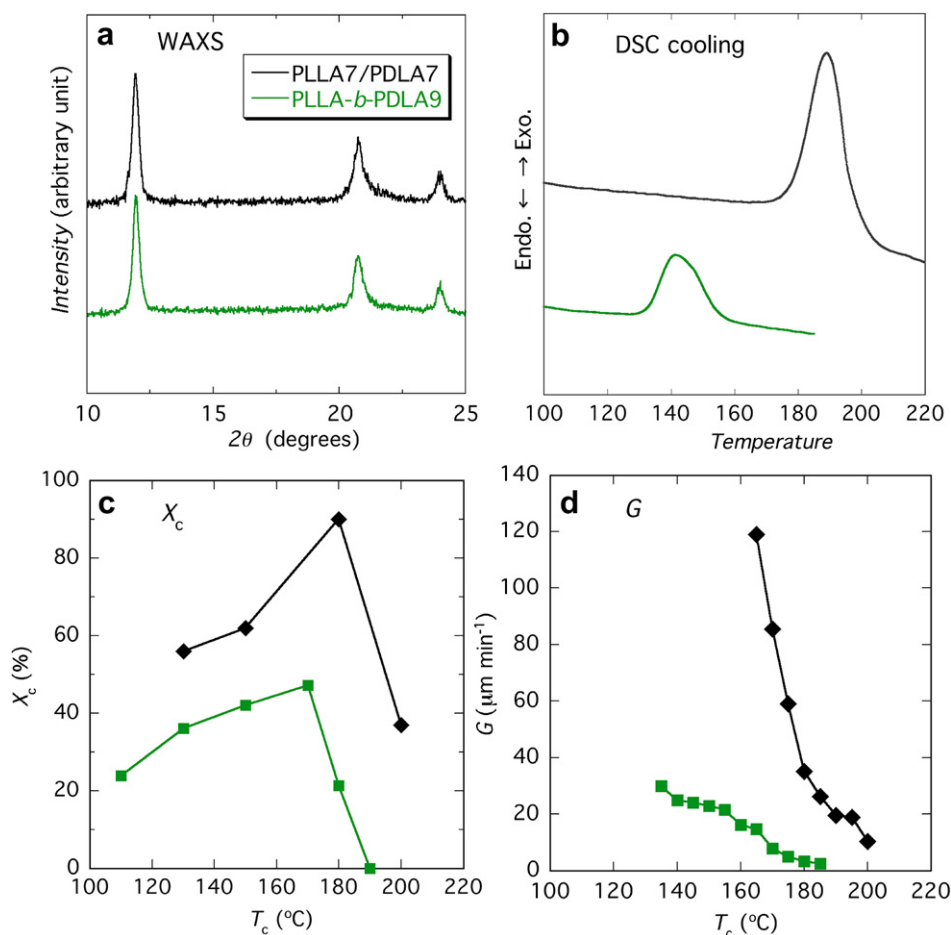| Code	G_0 (μm min^{-1})	K_g (K^2)	Regime
PLLA3	9.27×10^9	3.93×10^5	III
PLLA9	1.15×10^8	2.57×10^5	II
PLLA14	9.60×10^7	2.56×10^5	II
PLLA-*b*-PDLA4	1.15×10^{15}	1.29×10^6	–
PLLA-*b*-PDLA9	5.78×10^{10}	7.72×10^5	–
PLLA-*b*-PDLA11	2.31×10^{12}	9.66×10^5	–
PLLA7/PDLA7	8.93×10^8	5.00×10^5	–

3.3.4. Nucleation and front constants

We estimated the nucleation constant (K_g) and the front constant (G_0) for the PLLA homopolymers and the PLLA-*b*-PDLA copolymers by the use of the nucleation theory established by Hoffman et al. [37,38], in which G can be expressed with the following equation:

$$G = G_0 \exp[-U^*/R(T_c - T_\infty)]\exp[-K_g/(T_c\Delta Tf)] \quad (4)$$

where ΔT is the degree of supercooling $T_m^0 - T_c$, T_m^0 is equilibrium T_m, f is the factor expressed by $2T_c/(T_m + T_c)$ that accounts for the change in heat of fusion as the temperature is decreased below T_m^0, U^* is the activation energy for the transportation of segments to the crystallization site, R is the gas constant, and T_∞ is the hypothetical temperature at which all motion associated with viscous flow ceases. Fig. 10 illustrates the ln G + 1500/$R(T_c$-$T_\infty)$ of the PLLA homopolymers and the PLLA-*b*-PDLA copolymers as a function of $1/(T_c\Delta Tf)$. Here, we used 212 °C as the T_m^0 of the homo-crystallites of the PLLA homopolymers [30] and 279 °C as the T_m^0 of the stereocomplex crystallites of the PLLA-*b*-PDLA copolymers for comparison between the present and the reported studies, and the T_g values of the melt-quenched polymers in the present study. Also, we used the universal values of $U^* = 1500$ cal mol^{-1} and $T_\infty = T_g - 30$ K, as used in the reported literature [20,39–44].

The plots in this figure gives K_g values as slopes and intercepts ln G_0. The thus estimated values are given in Table 3. From the K_g values, we can obtain information about the crystallite growth mechanism [45]. Normally, crystallite growth mechanisms are classified into three regimes, i.e., Regimes I, II, and III, depending on T_c and consequently on the ratio of the lateral growth rate (g) to the rate of formation of secondary nuclei (i). The ratio of g to i increases with an increase in T_c. Regimes I, II, and III are respectively observed for high, middle, and low T_c and the ratio of g to i. Also, the relationship of K_g with Regime I and III is twice that with Regime II kinetics. Therefore, the K_g value difference indicates the difference in the crystalline growth mechanism. The K_g values of 2.6×10^5 K^2 for PLLA9 and PLLA14 homopolymers are very similar to those previously reported for PLLA in regime II kinetics ($2.2-2.6 \times 10^5$ and K^2) [39,41,42], whereas the PLLA3 homopolymer had a higher K_g value (3.9×10^5 K^2). This strongly suggests that the crystallization of

Fig. 11. WAXS profiles (T_c = 130 °C) (a), DSC thermograms during cooling from the melt (b), X_c (c), and G (d) of blend of PLLA7 (M_n = 7.1 × 10^3 g mol^{-1}, M_w/M_n = 1.2) and PDLA7 (M_n = 6.7 × 10^3 g mol^{-1}, M_w/M_n = 1.2), together with those of the PLLA-*b*-PDLA9 copolymer (having the highest crystallizability among the PLLA-*b*-PDLA copolymers). The upper and lower data in parts (a)–(d) are respectively those for the PLLA7/PDLA7 blend and the PLLA-*b*-PDLA9 copolymer.

the PLLA9 and PLLA14 homopolymers and of the PLLA3 homopolymer proceeded via Regime II and III kinetics, respectively. In contrast, because the K_g values of the PLLA-b-PDLA copolymers (7.7×10^5–1.3×10^6 K^2) were higher than those for Regimes II and III of the PLLA homopolymers, we could not specify the regime of the PLLA-b-PDLA copolymers.

The G_0 value of the PLLA3 homopolymer (9.3×10^9 μm min^{-1}) is slightly lower than the reported value (1.8×10^{10}–5.3×10^{11} μm min^{-1}) for PLLA in Regime III kinetics and those of PLLA9 (1.2×10^8 μm min^{-1}) and PLLA14 (9.6×10^7 μm min^{-1}) homopolymers are slightly higher than the reported values (2–4×10^7 μm min^{-1}) for PLLA in Regime II kinetics [41,42]. The G_0 value of the PLLA-b-PDLA9 copolymer (5.8×10^{10} μm min^{-1}) is comparable with those reported for PLLA, whereas the G_0 values of the PLLA-b-PDLA4 (1.2×10^{15} μm min^{-1}) and PLLA-b-PDLA11 (2.3×10^{12} μm min^{-1}) copolymers are higher than those reported for PLLA.

3.4. Comparison with polymer blend

Comparison of the crystallization behavior of the PLLA-b-PDLA copolymers with the PLLA/PDLA blend should be crucial in terms of commercial applications. Fig. 11 shows the WAXS profile, X_c and G for isothermal crystallization, and DSC thermograms during cooling of a PLLA7/PDLA7 blend, together with those of the PLLA-b-PDLA copolymer having the highest crystallizability, i.e., the PLLA-b-PDLA9 copolymer. Here, it should be noted that each polymer molecular weight of the PLLA7/PDLA7 blend is similar to the total molecular weight of the PLLA-b-PDLA9 copolymer but is higher than the block molecular weight of the PLLA or PDLA chain in the PLLA-b-PDLA9 copolymer. The PLLA7/PDLA7 blend had sufficiently low molecular weights to form only stereocomplex crystallites as crystalline species, which is evident from the similar diffraction profiles of the blend and the PLLA-b-PDLA9 copolymer [Fig. 11a].

The PLLA7/PDLA7 blend had much higher X_c and G values compared to those of the PLLA-b-PDLA9 copolymer [Fig. 11b and c]. Although the T_{cc} values during heating are similar for the PLLA7/PDLA7 blend and the PLLA-b-PDLA9 copolymer, the T_m values during heating, the ΔH_{cc} values during heating and cooling, and the T_{cc} values during cooling were higher for the PLLA7/PDLA7 blend than for the PLLA-b-PDLA9 copolymer (Table 2). These findings indicate that the connection between the PLLA and PDLA segments disturbed the free movement of PLLA and PDLA chains of the block copolymers during crystallization. However, the lower T_m of the PLLA-b-PDLA9 copolymer can be ascribed to the fact that its PLLA and PDLA chains are shorter compared to those of PLLA7 and PDLA7, which may have reduced the upper limit of crystalline thickness. The higher T_m value of the PLLA7/PDLA7 blend compared to that of the PLLA-b-PDLA9 copolymer induced the larger ΔT during cooling from the melt. This should be the cause for the higher T_{cc} of the PLLA7/PDLA7 blend.

The K_g value of the PLLA7/PDLA7 blend was estimated by the same procedure for the PLLA-b-PDLA copolymers. The obtained K_g value (5.0×10^5 K^2), which is slightly lower than those reported for PLLA/PDLA blends (9.0×10^5–1.2×10^6 K^2), probably because of their lower M_n values of 2.7 and 3.9×10^3 g mol^{-1} [44], is lower than those of the PLLA-b-PDLA copolymers (7.7×10^5–1.3×10^6 K^2) (Table 3), suggesting that the crystallite growth mechanism of the PLLA7/PDLA7 blend is different from that of the PLLA-b-PDLA copolymers. On the other hand, the G_0 value of the PLLA7/PDLA7 blend (8.9×10^8 μm min^{-1}), which is lower than those reported for PLLA/PDLA blends (1.0×10^{12}–1.2×10^{14} μm min^{-1}), probably because of their low M_n values [44], is comparable with those of the PLLA homopolymers (9.6×10^7–9.3×10^9 μm min^{-1}) but lower

than those of the PLLA-b-PDLA copolymers (5.8×10^{10}–1.2×10^{15} μm min^{-1}) (Table 3).

4. Conclusions

The conclusions derived from the present study on the stereocomplex crystallization and spherulite growth behavior of PLLA-b-PDLA copolymers are summarized as follows:

(1) For isothermal and non-isothermal crystallization, only stereocomplex crystallites as crystalline species were formed in all PLLA-b-PDLA copolymers with M_n of 3.9×10^3–1.1×10^4 g mol^{-1}, causing higher T_m of the PLLA-b-PDLA copolymers.

(2) For non-isothermal crystallization, the T_{cc} values of the PLLA-b-PDLA copolymers during heating and cooling were respectively lower and higher than those of the PLLA homopolymers, indicating accelerated crystallization of the PLLA-b-PDLA copolymers.

(3) For isothermal crystallization, in the crystallizable T_c range, the X_c values of the PLLA-b-PDLA copolymers were lower than those of the PLLA homopolymers and were susceptible to the effect of T_c compared to that of the PLLA homopolymers.

(4) The G of the PLLA-b-PDLA copolymers decreased with an increase in T_c. The G values were highest for the PLLA-b-PDLA copolymer having a middle (not the lowest) M_n of 9.3×10^3 g mol^{-1} (PLLA-b-PDLA9). This trend is different from that of the PLLA homopolymers where the G values increased monotonically with a decrease in M_n, and seems to be caused by the upper critical M_n values of PLLA and PDLA chains, as in the case of PLLA/PDLA blends (in other papers), above which homo-crystallites are formed in addition to stereocomplex crystallites.

(5) The disturbed crystallization of the PLLA-b-PDLA copolymer compared to that of the PLLA/PDLA blend is attributable to the segmental connection between the PLLA and PDLA chains, which interrupted the free movement of the PLLA and PDLA chains of the PLLA-b-PDLA copolymers during crystallization. The crystallite growth mechanism of the PLLA-b-PDLA copolymers was different from that of a PLLA/PDLA blend.

References

[1] Ikada Y, Jamshidi K, Tsuji H, Hyon S-H. Macromolecules 1987;20:904–6.
[2] Slager J, Domb AJ. Adv Drug Deliv Rev 2003;55:549–83.
[3] Tsuji H. Macromol Biosci 2005;5:569–97.
[4] Fukushima K, Kimura Y. Polym Int 2006;55:626–42.
[5] Tsuji H, Ikada Y. In: Yu L, editor. Biodegradable polymer blends and composites from renewable resources. NJ: Wiley; 2008. p. 165–90 [Chapter 7].
[6] Kakuta M, Hirata M, Kimura Y. Polym Rev 2009;49:107–40.
[7] Yui N, Dijkstra PJ, Feijen J. Makromol Chem 1990;191:481–8.
[8] Spassky N, Wisniewski M, Pluta C, Le Borgne A. Makromol Chem Phys 1996;197:2627–37.
[9] Spinu M, Jackson C, Keating MY, Gardner KH. J Macromol Sci Part A Pure Appl Chem 1996;33:1497–530.
[10] Sarasua J-R, Prud'homme RE, Wisniewski M, Le Borgne A, Spassky N. Macromolecules 1998;31:3895–905.
[11] Ovitt TM, Coates GW. J Am Chem Soc 2000;124:1316–26.
[12] Li L, Zhong Z, De Jeu WH, Dijkstra PJ, Feijen J. Macromolecules 2004;37:8641–6.
[13] Hu J, Tang Z, Qiu X, Pang X, Yang Y, Chen X, et al. Biomacromolecules 2005;6:2843–50.

[14] Tang Z, Yang Y, Pang X, Hu J, Chen X, Hu N, et al. J Appl Polym Sci 2005;98:102–8.
[15] Fukushima K, Furuhashi Y, Sogo K, Miura S, Kimura Y. Macromol Biosci 2005;5:21–9.
[16] Fukushima K, Kimura Y. J Polym Sci Part A Polym Chem 2008;46:3714–22.
[17] Kim SH, Nederberg F, Zhang L, Wade CG, Waymouth RM, Hedrick JL. Nano Lett 2008;8:294–301.
[18] Nederberg F, Appel E, Tan JPK, Sung HK, Fukushima K, Sly J, et al. Biomacromolecules 2009;10:1460–8.
[19] Hirata M, Kobayashi K, Kimura Y. J Polym Sci Part A Polym Chem 2010;48: 794–801.
[20] Tsuji H, Sugiura Y, Sakamoto Y, Bouapao L, Itsuno S. Polymer 2008;49: 1385–97.
[21] Tsuji H, Nakano M, Hashimoto M, Takashima K, Katsura S, Mizuno A. Biomacromolecules 2006;7:3316–20.
[22] Tsuji H, Del Carpio CA. Biomacromolecules 2003;4:7–11.
[23] Fox TG, Loshaek S. J Polym Sci 1955;15:371–90.
[24] Flory PJ. J Chem Phys 1949;17:223–40.
[25] Jamshidi K, Hyon S-H, Ikada Y. Polymer 1988;29:2229–34.
[26] Bouapao L, Tsuji H, Tashiro K, Zhang J, Hanesaka M. Polymer 2009;50: 4007–17.
[27] Alamo RG, Viers BD, Mandellkern L. Macromolecules 1995;28:3205–13.

[28] Marand H, Xu J, Srinivas S. Macromolecules 1998;31:8219–29.
[29] Tsuji H, Ikarashi K. Biomacromolecules 2004;5:1021–8.
[30] Tsuji H, Ikada Y. Polymer 1995;36:2709–16.
[31] Tsuji H, Ikada Y. J Polym Sci Part A Polym Chem 1998;36:59–66.
[32] Tsuji H, Ikada Y. Polym Degrad Stab 2000;67:179–89.
[33] Tsuji H, Ikarashi K. Polym Degrad Stab 2001;71:415–24.
[34] Abe H, Kikkawa Y, Inoue Y, Doi Y. Biomacromolecules 2001;2:1007–14.
[35] Tsuji H, Ikada Y. Macromol Chem Phys 1996;197:3483.
[36] Tsuji H, Tsuruno T. Polym Degrad Stab 2010;95:477–84.
[37] Hoffman JD, Davis GT, Lauritzen JI. Treatise on solid state chemistry. In: Hannay NB, editor. Crystalline and noncrystalline solids. New York: Plenum Press; 1976. vol. 3, [Chapter 7].
[38] Hoffman JD, Davis GT, Lauritzen JI. J Res Nat Bur Std-A Phys Chem 1975;79A: 671–99.
[39] Vasanthakumari R, Penning AJ. Polymer 1983;24:175–8.
[40] Tsuji H, Tezuka Y. Biomacromolecules 2004;5:1181–6.
[41] Tsuji H, Tezuka Y, Saha SK, Suzuki M, Itsuno S. Polymer 2005;46:4917–27.
[42] Tsuji H, Miyase T, Tezuka Y, Saha SK. Biomacromolecules 2005;6:244–54.
[43] Abe H, Harigaya M, Tsuge T, Doi Y. Biomacromolecules 2005;6:457–67.
[44] Bouapao L, Tsuji H. Macromol Chem Phys 2009;210:993–1002.
[45] See for example Gedde UW. Polymer physics. London: Chapman & Hall; 1995. Chapters 7 and 8, pp. 169–198.